PAPER • **OPEN ACCESS**

Synthesis and characterization of the microcellular injection molded PA6/flax and the PA6/graphene nanocomposites

To cite this article: Ming-Wei Shao *et al* 2019 *IOP Conf. Ser.: Mater. Sci. Eng.* **542** 012067

IOP Conf. Series: Materials Science and Engineering **542** (2019) 012067 doi:10.1088/1757-899X/542/1/012067

Synthesis and characterization of the microcellular injection molded PA6/flax and the PA6/graphene nanocomposites

Ming-Wei Shao[1], Jung-Jie Huang[1], Yu-Xuan Chen[2] and Shyh-Shin Hwang[2,*]

1 Da-Yeh University, Chang-hwa, Taiwan.

2 Chien-Hsin University of Science and Technology, Jhongli, Taiwan.

E-mail: stanhwang@uch.edu.tw

Abstract. Polymer composites combine two materials together to produce a unique property which is not inherent to the individual materials. The most important reason to use composites is the enhancement of the mechanical properties. However, there are several applications that can be used by composites, such as the heavy metal adsorption of waste water by flax. This study has investigated the effects of flax (1, 3, 5 wt%) and graphene loading (0.5, 1, 3 wt%) on the tensile strength, thermal, and heavy metal adsorption properties of the microcellular injection molded PA6 composites. The fillers used, flax and graphene, were micro and nano materials in size, respectively. The results showed that the dispersion with 0.5 wt% of graphene loading, as seen in the TEM pictures, had the best dispersion for the PA6/graphene nanocomposites. This amount of graphene also had the best tensile strength in three different loadings (0.5, 1.0, 3.0 wt%). Tensile strength was related to the filler dispersion in the matrix. Good dispersion resulted in good tensile strength, and the elongation decreased by increasing the flax loading. The 5 wt% flax loading and 3 wt% graphene loading of the composites showed the largest storage modulus for the PA6composites. The 1 wt% of the flax loading showed the highest degradation temperature for the PA6/flax micro-composites, and the 3 wt% for the PA6/graphene nanocomposites. The cell size decreased and the cell density increased with the addition of graphene to the PA6 composites. Heavy metal of the Cr(IV)adsorption test showed that the PA6/GP nanocomposites had a better adsorption than that of the PA6/flax composites.

1. Introduction

The filler has several functions, e. g., reinforcements [1], flame resistance [2], cost reduction [3], thermal stability [4], and a toughness modifier [5].Since the introduction of polymer which replaced the metal and non-metal in many household applications however, polymer strength is not good enough to sustain the external load as compared to those of the metal and non-metal materials. Hence,fiber reinforced polymers were used to improve the matrix strength. There are several types of reinforced fillers, e.g. glass fiber, carbon fiber[6], and aramids fiber. They have wide applications, especially in the aerospace and automobile industry. However, those fibers are not environmentally-friendly. So the natural fibers as the reinforcement of the polymer are more popular. People had used fibers extracted from animals or plants before the synthetic fiber was discovered in 1885. The most common natural fibers are from cotton, hemp, silk, and fur. Hemp fiber like flax, cannabis, and jute, possess the antibacterial characteristics and are green fibers. Flax fibers are mostly composed of cellulose and hemicellulose. Flax fiber is extracted from the bast beneath the surface of the stem of the flax plant. Flax fiber is soft, lustrous, and not easy to corrode. Zampaloni et al., [7]

used marijuana, flax, sisal, mestha, and coir fiber as the reinforcement for the PP matrix and compared the mechanical property between them. Maleic anhydride (MA) was used as the grafted agent. The results showed that marijuana, flax, and sisal had better properties that those of mestha and coir fiber. A coupling agent of silane [8, 9] was used to modify the flax fiber since it is hydrophilic.

Graphene (GP),two-dimensional, materials have attracted tremendous research interest due to their remarkable physio-chemical properties including electrical, mechanical, and thermal. Thus, a combination of different beneficial properties makes GP an ideal candidate for polymer nanocomposites and nanotechnology.GP dramatically improves the properties of polymer based composites at a very low loading point, and the most fascinating attribute is the very high surface conductivity leading to the formation of numerous electrically conductive polymer composites [10-9].Polymer/GP nanocomposites are formed when the polymer and GP nanofiller (graphene oxides [13], reduced graphene oxides [14], chemically reduced graphene oxide, and thermal reduced graphene oxides etc.) are mixed via various methods, such as in situ, polymerization, solution blending, and melt blending. Among these different processes, most of the polymer/GP nanocomposites were produced by melt blending because it is a commercially feasible, lower cost, environmentally friendly, and straightforward approach that does not involve any solvents or monomers [15]. Melt blending is accepted as being the most researched and developed method within the industry.

Water pollution is one of the most serious problems worldwide. In particular, the toxic metals in drinking water pose a huge challenge to the globalmunicipalities. Heavy metals are toxic to plants, animals, human beings, and aquatic life, hence the reason why they have attracted so much attention.Sources of heavy metal pollutants include industrial wastewater from mining, metal processing, and tannery, pharmaceutical and chemical engineering industries, and if the metal ions are not removed fromthe wastewater they may bring long-term risks to the environment. Water treatment such as precipitation, ionic exchange, and adsorption [16-18] has been previously used to remove heavy metals from the aqueous solution. Among them, adsorption receives considerable interest in heavy metal removal because of its high adsorption efficiency, easy handling, cost effectiveness, and the availability of different adsorptive materials [19-21].

In this research, we have investigated the microcellular injection molding process as a commercially useful and valuable technique for improving the shrinkage/warpage of the plastics. The study has focused on the effects of the fillers loading on the structure, thermal, tensile, and the heavy metal adsorption properties of the microcellular injection molded PA6/flax and the PA6/GF composites. The primary purpose of the research was to investigate the processing benefits and property variances by micro and nano composites.

2. Materials and methods

2.1. Materials

Micro-sizedflax fiber with an L/D ratio of 2000 and a diameter of 10μm was supplied by the Shan-yuan Co. of Taiwan. Graphene, HGN-8, with a diameter of 8 μm and a thickness of 100 nm, and micromechanical exfoliation from Graphite was used. PA6, type 2100 with a melt flow index of 45 g/10minwas purchased from the Nan-Ya Plastics Corporation, Taiwan.

2.2. Compounding and foaming process

The PA6/flax and the PA6/graphene composites were preparedthrough the blending of the flax and graphene with the PA6resin using a twin-screw extruder. The loadings of the flaxwere 1, 3, and 5 wt%,and 0.5, 1.0, and 3.0wt% for the graphene. Then, the micro compositeswere molded separately usingthe conventional and Mucell®injection molding processes. TheMucell®injection molding process was performed on a 100 ton ARBURG-420C injection molding machine, equipped with a microcellular foamingsystem. Nitrogen was used as a physical blowing agent in the foaming process. The injection molding setup is as shown in Figure 1. The processing parameters for both the conventional and Mucell® moldingare presented in Table 1.

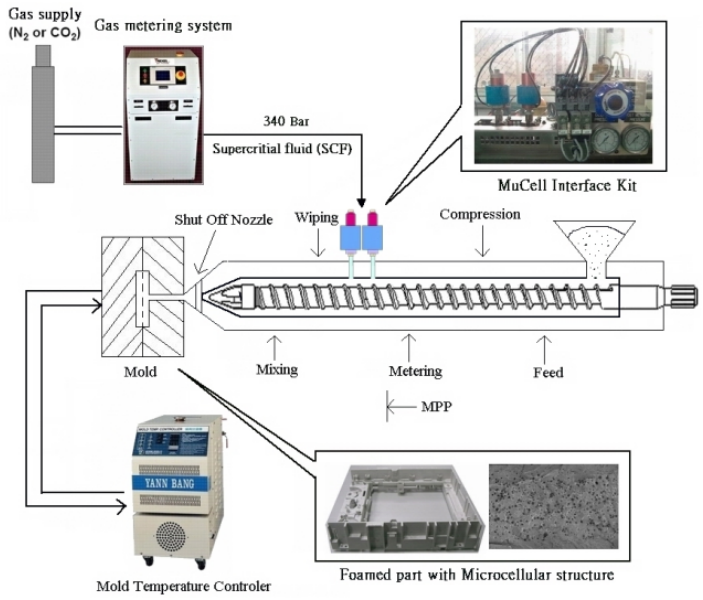

Figure 1. Microcellular injection molding setup.

Table 1. Process parameters both for conventional and Mucellinjectionmolding processes

Process parameters	PA6/flax and GP (Unfoamed)	PA6/flax and GP (Foamed)
Shot size (cm^3)	19	17
Melt temperature (°C)	290	290
Mold temperature (°C)	90	90
Injection speed (cm^3/s)	140	150
Injection pressure (bar)	1000	1000
Packing pressure (bar)	700	50
Back pressure (bar)	50	110
Screw speed (m/min)	20	20
Cooling time (s)	25	25
SCF content (wt %)	–	0.4
SCF flow rate (kg/h)	–	0.17

2.3 Instrumentations

The cellular structures of the foamed compositeswere examined usinga JEOL JSM6360scanning electron microscope (SEM) system. Specimens were cut into small pieces and sputter coated with gold before examining with the SEM. The transmission electron microscopy (TEM), was obtained on a JEOL JSM 6500F, and Model JEOL JEM2010, 200 kV, respectively. The sample thickness of 80 nm was prepared by using a Leica Ultracut-UCT to verify the physicochemical properties of the layer materials.Differential scanning calorimetry (DSC) analysis was used to study the thermal properties of the composites. The thermal analysis was performed using DSC technique (DSC821e, Mettler Toledo). Temperature range was 30–300 ℃ at the heating rate of 4℃/min. The thermal decomposition temperature was determined by thermosgravimetric analysis (TGA) (SII TG/DTA6200), and the experiment was performed by samples (10 mg) of air gas flow from 40ºC to 900ºC at a heating rate of 10ºC min^{-1}.Dynamic mechanical analysis (DMA) was performed using Perkin Elmer DMA 8000.

The molded samples were subjected to the tensile (ASTM Standard D638-02) examination. The reported mechanical properties data were the average of five successful tests.The tensile tests of the ASTM standard samples were carried out using a tensile test analyzer andan HT-9102M system(Hong-Da Company).

3. Results and discussion

This study aims to investigate the relationships and comparison between the processing, morphology, and the properties of the foamed PA6/flax and the PA6/GPnanocomposites produced bythe microcellular injection molding process.

3.1. Morphology of PA6/graphene nanocomposites and PA6/flax composites

The morphology of the PA6/GP was characterized by the XRD, TEM, and SEM analysis. The morphology of the PA6/flax was characterized by the SEM only. The XRD patterns of the nanocomposites are as shown in figures2(A) and (B). The XRD determines the change of the interlayer distance of the layered material. The characteristic basal peak of grapheneshowed at 26.47 degreecorresponding to 0.34 nm layer spacing at (0 0 2) direction. A higher content of graphene increases the intensity peak of the polymer which shows the graphene is more oriented [23]. From the XRD results, it is evident that the graphene is intercalated in the polymer matrix [24].

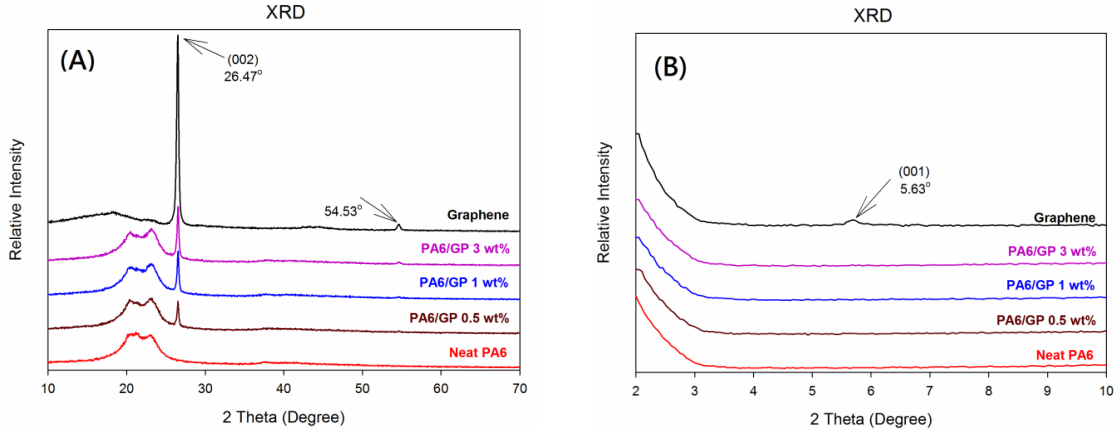

Figure 2: XRD pattern of PA6/graphene nanocomposites.

The XRD analysis alone is not sufficient to prove either intercalated or exfoliation morphology,thus the nanocomposites morphology was confirmed by the TEM analysis. The TEM pictures of the PA6/GP0.5 and 3.0 wt% nanocomposites (Figure 3 (A), (B), (C) and (D)) showall possible platelet morphologies, dramatically intercalated and stacked structures in a polymer matrix. The graphene thickness is around 100 nm.

Figures 4a and 4b show the typical SEM images of the fracture surfaces perpendicular to the melt flow direction obtained from the foamed PA6/flax and the PA6/GP composites. From the images, it is confirmed that the effects of the flax and GP on both the cell density and size of the foamed samples. The cell size of the neat PA6 is large and the quantity is in a small amount. The cell size is 47.89 µm for the neat PA6 and is 64.67, 32.09, and 48.92 µm for the flax loading of 1, 3, and 5 wt%, respectively (Figure 3a).The cell size is 47.89 µm for the neat PA6, and is 28.64, 16.72, and 14.36 µm for the GP loading of 0.5, 1.0, and 3.0 wt%, respectively, (Figure 3b). The cell size and density are in Tables 2 and 3 for the PA6/flax and PA6/GP nanocomposites, respectively. The GP nanocomposites havea smaller cell size, in that it has a more specific surface than that of the flax composites. When the GP content increased, the cell size decreased, and the cell density increased. Further, the decrease of the cell size also affected the tensile strength. This can be confirmed with the tensile strength from Figure 5. These results indicate that the flax rod and the GP layer served as the heterogeneous nucleating sites during the foaming process. In this heterogeneous nucleating system, filler particles and cells nucleate at the boundary between the polymer matrixes. The remarkable increase in the cell density of the composites is attributed to in the effectiveness of the nucleating sites either on the flax or GP layer surfaces. However,

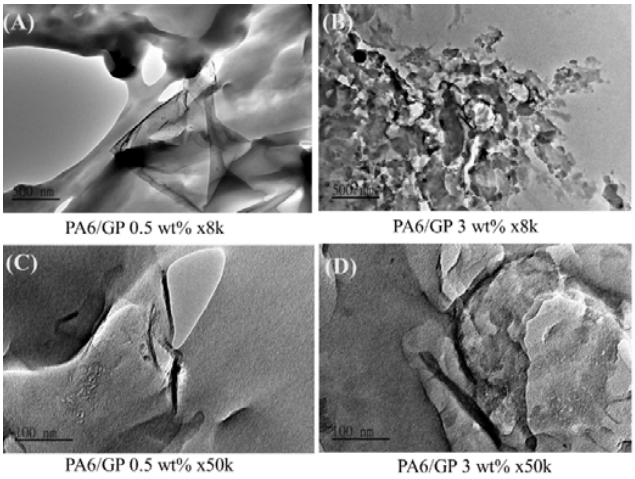

Figure 3.TEM images of PA6/graphene nanocomposites with different graphene loadings and magnifications.

the cell size leveled off when the MMT content was greater than 1 wt%. Upon the foam injection molding, bubble nucleation occurred at around 2 or 3 sec after the pressure started descending. In order to evaluate the effect of clay on the bubble nucleation and growth, the pressure profile has to be carefully controlled for every experiment to realize the same pressure conditions. The variability of the pressure profile at around 2 to 4 sec was less than 0.2 MPa among all the experiments.

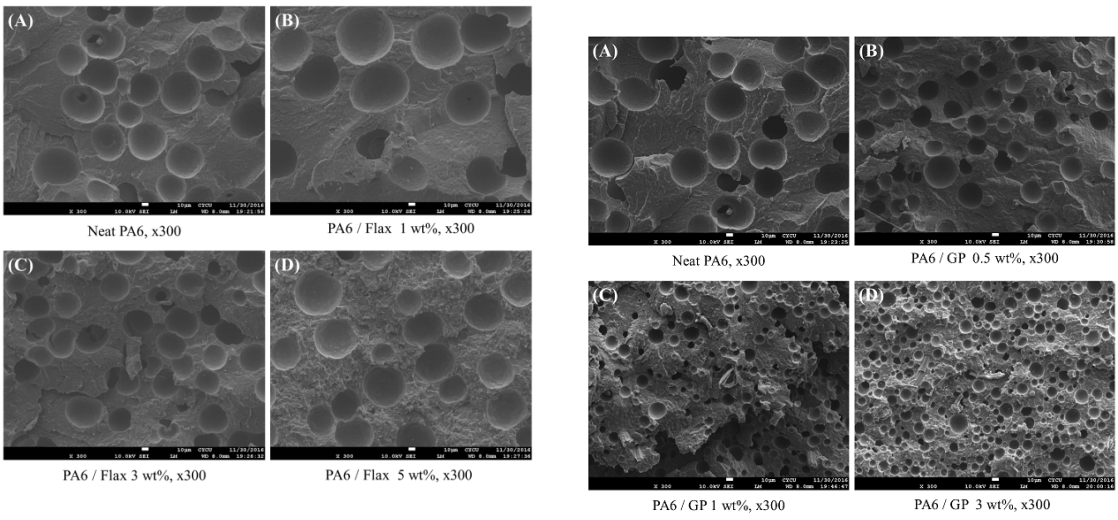

Figure 4.SEM images of the fracture surfaces perpendicular to the melt flow direction. (a) PA6/flax composites (b) PA6/GP nanocomposites.

Table 2. Cell size and cell density for PA6/flax composites.

Loading	Cell Size (μm)	Cell Density (Quantity/cm^3)
0 wt%	47.89	1.33 x10^{12}

1wt%	64.67	4.70 x10^{11}
3 wt%	32.09	2.69 x10^{12}
5 wt%	48.92	8.36 x10^{11}

Table 3. Cell size and cell density for PA6/GP nanocomposites.

Loading	Cell Size (μm)	Cell Density (Quantity/cm^3)
0 wt%	47.89	1.40 x10^{12}
0.5wt%	28.64	3.86 x10^{12}
1 wt%	16.72	2.22 x10^{13}
3 wt%	14.36	4.66 x10^{13}

3.2. Tensile Property

The purpose of adding the filler into the polymer is the tensile strength enhancement of the polymer matrix for most of the composites. The shape (rod, plate, and sphere) and the L/D ratio of the filler playan important role on the strength enhancement. The interface (untreated or treated filler) between the filler and matrix is also an important issue. Figures5(a) and (b) shows the load-displacement of the foamed PA6/flax composites and the PA6/GP nanocomposites, respectively. Figure 5(a) showsthe decreasedtensile strength and elongation with the addition of the flax filler. The tensile strength was1637.9, 1641.6, 1542.0, and 1414.0 Nfor the neat PA6, 1, 3,and 5wt% flax, respectively. Elongation was 66.4, 42.0, 26.9, and 16.0% for the neat PA6, 1, 3, and 5wt% flax, respectively. However, it has a different trend for the PA6/GP nanocomposites. The tensile strength increased then leveled off at 3 wt of the GP loading.The tensile strength was 1453.35,1644.1,1493.47, and 1266.17 Nfor the neat PA6, 0.5, 1,and3 wt% of the GP loading, respectively.

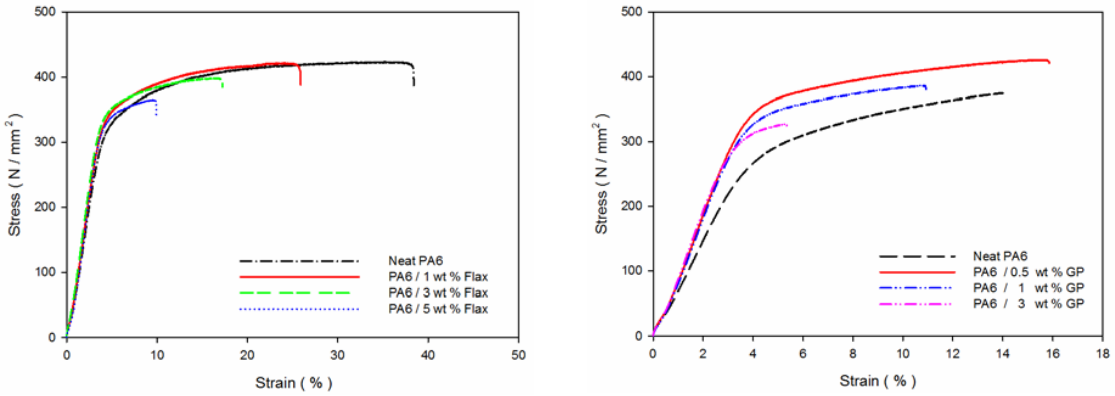

Figure 5. Load displacement curves of PA6/flax and PA6/GP nanocomposites.

3.3 Thermal Property

3.3.1 TGA

The TGA results of the nanocomposites are as shown in Figures 6 (a) and (b). The thermal stability ofthe PA6/flax composites andthe thermal decomposition temperature (Td) were increased as compared to that of the pure polymer. The peak degradation temperature of the PA6/flax compositeswas found to increase to 4.7°C, from 470.3 to 475.5°C. Whereasthe flaxfiller acts as a thermal retardant, also the enhanced thermal stability were attributed to the homogeneous dispersion of the flaxfiller in the polymer matrix. While the thermal decomposition temperature decreased for the PA6/GP nanocomposites.This is caused by the poor interface bonding between the GP and the PA6 matrix.

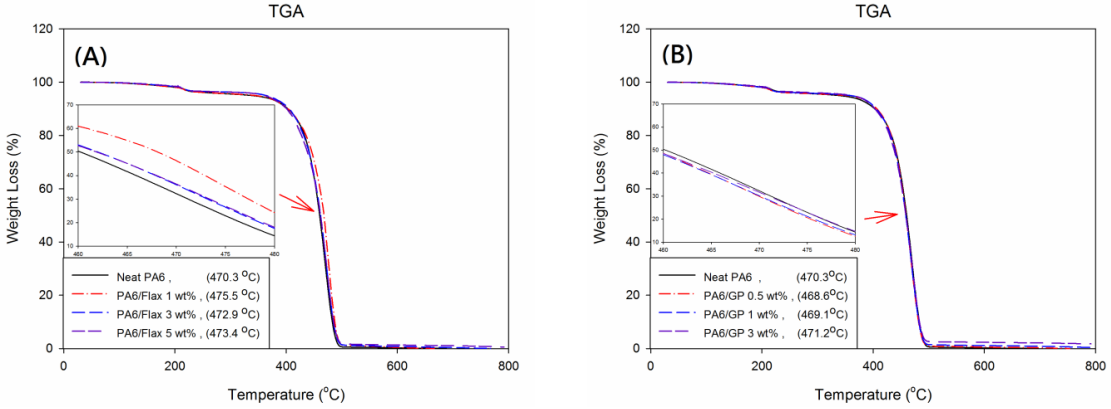

Figure 6.TGA results of (a) PA6/flax and (b) PA6/GP nanocomposites.

3.3.2 DSC

The DSC thermograms of the nanocomposites are shown in figures 7, and 8,and the melting temperature (*Tm*) and the cooling crystal temperature (Tcc) of the polymer nanocomposites. It was observed that the polymer nanocomposites Tm were almost similar after the addition of either the flax or GP in both the polymer composites. But the Tcc were higher for the GP filler than that of the flax filler indicating the GP helped the crystallization. However, the increased concentration of the micro or nano-fillers leads to the decrease of the crystallinity of the nanocomposites. This is caused by the foaming process [25].

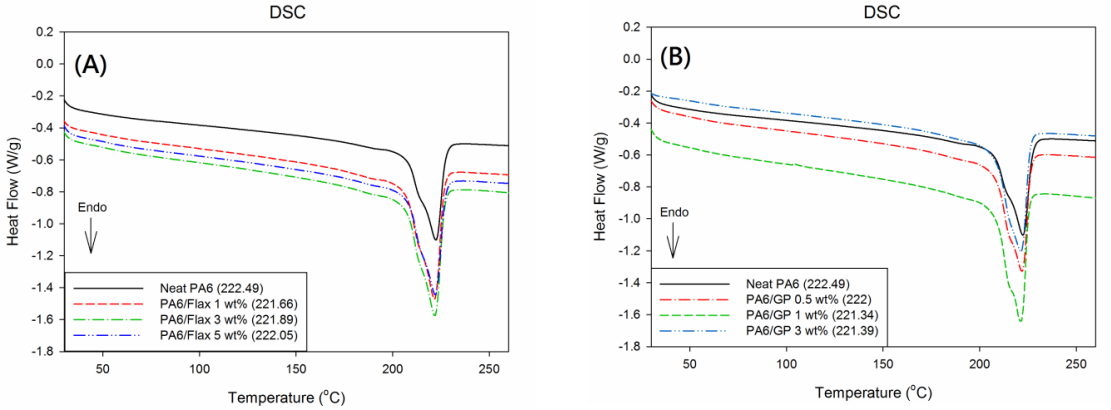

Figure 7. Heating curves of DSC for (a) PA6/flax and (b) PA6/GP nanocomposites.

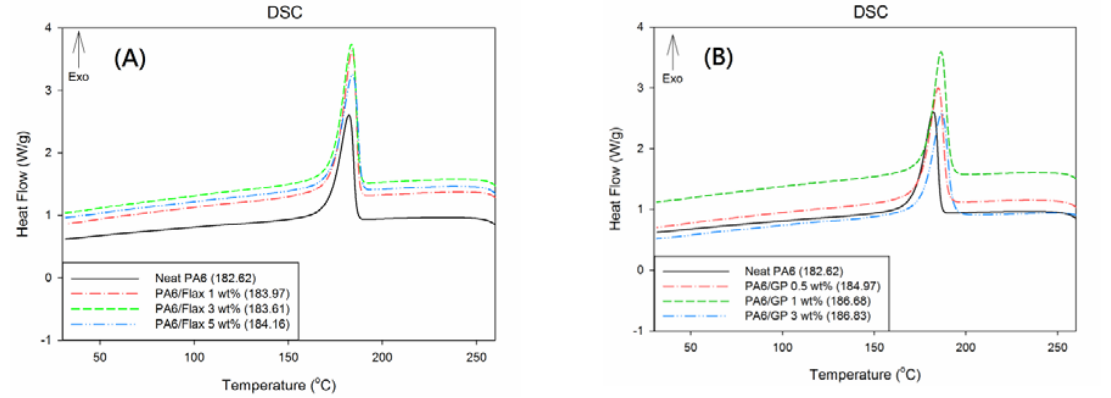

Figure 8. Cooling curves of DSC for (a) PA6/flax and (b) PA6/GP nanocomposites.

Table 4. Thermal analysis of PA6/flax and PA6/GP nanocomposites

Filler (wt%)	Tm (℃)	△H (J/g)	Tcc (℃)	△Hc (J/g)	Xc (%)
Neat PA6	222.5	36.7	182.6	47.6	5.7
Flax 1	221.6	53.5	184.0	62.9	5.0
Flax 3	221.9	50.2	183.6	61.3	5.9
Flax 5	222.	48.1	184.2	55.8	4.2
GP 0.5	222	48.6	185.0	52.5	2.0
GP 1.0	221.34	49.94	186.68	53.62	1.96
GP 3.0	221.39	48.8	186.83	51.27	1.34

3.4 DMA

Figures 9 and 10 show the storage modulus and tan δ for the PA6/flax and the PA6/GP nanocomposites, respectively. The storage modulus can exhibit the stiffness of the material and tan δ indicates the glass transition temperature of the composites. The storage modulus is 2431, 2780, 2835, and 3065MPa at 60℃ for the neat PA6, 1, 3, 5 wt% flax, respectively. The storage modulus increases as the flax loading increases. While it is 2399, 2622, 2775, 3221 MPaat 60℃ for the neat PA6, 0.5, 1, 3 wt% GP, respectively. When comparing these two composites, the PA6/GP nanocomposites have a larger storage modulus than that of the PA6/flax composites. The glass transition temperature is not apparent for the PA6/flax composites as shown in Figure 9B. This can be verified in the TMA analysis section. The glass transition temperature is 70.4, 62.9, 60.6, and 58.6℃ for the neat PA6, 0.5, 1, 3 wt% GP, respectively, as shown in Figure 10b.

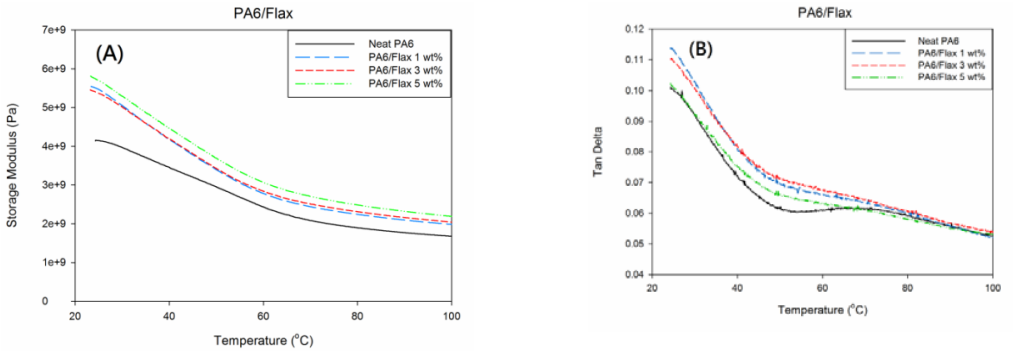

Figure 9. Storage modulus and Tanδof PA6/flax composites.

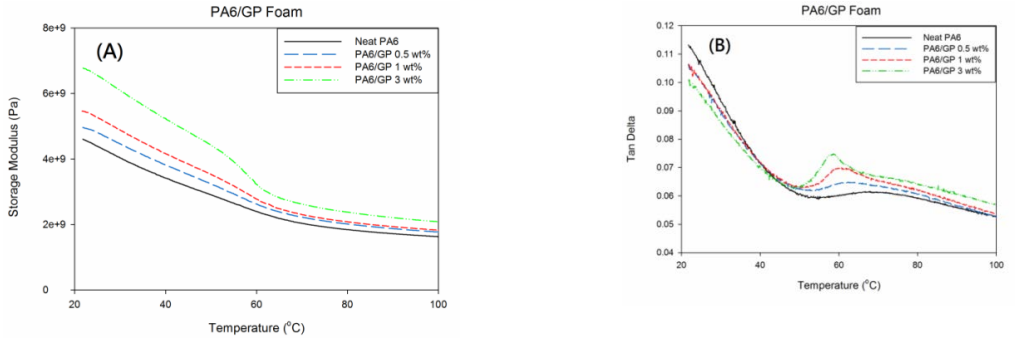

Figure 10. Storage modulus and Tanδ of A6/GP nanocomposites

3.5 Heavy metal adsorption

This adsorption study is based on the Langmuir isotherm. The Langmuir model has been established on the theory that a max adsorption arises when a saturated monolayer of solute molecules is existent on the adsorbent surface[26], also that the energy of the adsorption is continuous, and that there is no movement of the adsorbate particles on the surface plane. The effect of the filler content and the initial concentration on the percentage removal of the Cr(IV) by the PA6/flax composites and the PA6/GP nanocomposites areas shown in Figure 11, respectively. Figure 11a shows the effect of the filler content on the heavy metal removal. The results show that the GP has a better Cr(IV) adsorption than that of the flax. There were five different initial concentrations of the Cr(IV) chosen for the study, i.e. 10, 20, 30, 40 and 50 mg/l with a constant dose of 0.05 g of the adsorbent composites and nanocomposites. The ability of the PA6/flax and the PA6/GP composites to adsorb the Cr(IV) is attributed to the presence of the exchangeable ions, such as Si-O and Al-O, and also the swelling ability. The PA6/flax and the PA6/GP composites were able to adsorb almost 42% and 49%, respectively, of the Cr(IV) at 20 mg/l. The adsorption levels off when the concentration is higher than 20 mg/l, both for the PA6/flax and the PA6/GP nanocomposites.

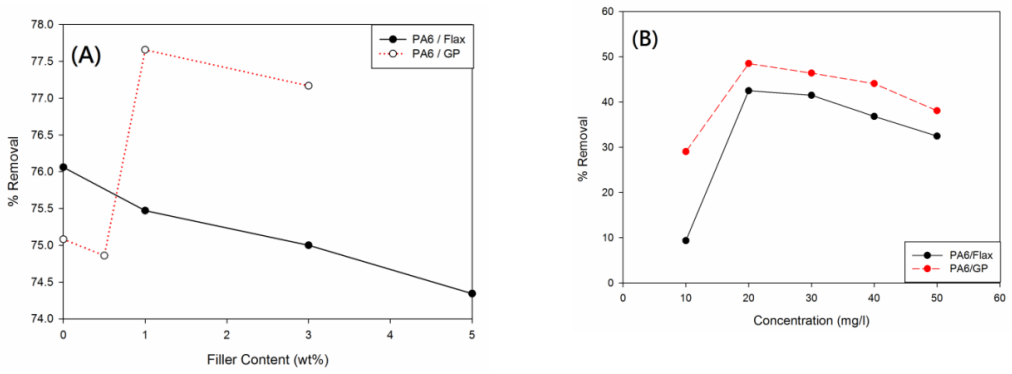

Figure 11. Heavy metal Cr (IV) adsorption test of PA6/flax and PA6/GP nanocomposites.

Acknowledgments
This study was supported by Ministry of Science and Technology, Taiwan under grant MOST 105-2923-E-231-001-MY3.

[1] TsaiT-Y, LinM-J, ChuangY-C, ChouP-C, 2013 *MCP*, **138**, *1, 230-237.*
[2] Chang, M-K, Hwang, S-S, Liu, S-P, 2014 *JIEC*,**20**, 4,25,1596.
[3] Katz H S, Mileski J V, 1988, *Handbook of Fillers for Plastics*, (New York: Springer) 5, pp 55
[4] Blanco I, Abate L, Antonelli M L, Bottino F A, Bottino P, 2012 *Express Polym Lett* **6**(12), 997-1006.
[5] Petrucci R and Torre L, 2017, Filled Polymer Composites, *Modification of Polymer Properties*,edCarlos Federico Jasso-Gastinel, José M. Kenny (New York: William Andrew), chapter 2, pp 28-2.
[6] LiuY, ZwingmannB,Schlaich M, 2015 *Polym*, **7**(10), 2078-2099.
[7] ZampaloniM, PourboghratF,YankovichSA, RodgersBN, MooreJ, DrzalLT, Mohanty AK, Misr M, 2007 *Compos Part Appls*, **38**(6), 1569-1580.

[8] YanjunX, CallumAS, Zefang X, Holger M, CarstenM, 2010*Compos Part A-Appls*, **41**(7), 806-819.
[9] Valadez-GonzalezA, CervantesR,OlayoPJ, HerreraF,1999 *Compos Part B-Eng*, **30**(3), 321–331.
[10] Reina A, Jia X T, Ho J, NezichD, Son H B, Bulovic V, Dresselhaus M S, Kong J, 2009 *Nano Lett*, **9**, 30.
[11]NovoselovKS, GeimK, MorozovSV, Jiang D, ZhangY, Dubonos S V, Grigorieva IV, Firsov AA, ,2004 *Science*, **306,** 666.
[12] WuMQ, XuY, YaoZ, LiuA, Shih G, 2010 *ACS Nano*, **4**, 1963.
[13] HummersWS,OffemanRE, 1958 *JACS*,**80** (6): 1339.
[14] WuZ-S, RenW, GaoL, LiuB, JiangC, ChengH-M, 2009 *Carbon*, **47**, 493.
[15] BunekarN, TsaiT-Y, YuY-Z, 2016 *Mater Today-Proc*, **3**, 1415.
[16] HuaM, ZhangS, PanB, Zhang W,LvL, Zhang Q,2012 *J. Hazard. Mater*, **211–212**, *317–331*
[17] TaghipourKolaeiZ,TanziM,YouseA, and EisazadehH, 2012*J. VinylAddit. Technol*, **18**, *52–56.*
[18] MittalB,and MishraS,2014 *CarbohydPolym*, **101**, 1255.
[19] VeliS,AlyüzB, 2007*J Hazard Mater*, **149**, 1, 226-233.
[20] ŞölenerM,TunaliS,ÖzcanA,GedikbeyT, 2008 *Desalination*, **223**, 1-3, 308-322.
[21] RožićM,Cerjan-StefanovićS, KurajicaS,VančinaV, 2000 *Water Res*, **34**, 14, 3675–3681.
[22] HastutiB, Masykur A, HadiS, 2016 *IOP Conf. Ser.: Mater. Sci. Eng.*,**107**, 012010.
[23] LiX-Y, WangZ-Z, WuL-X, TsaiT-Y, 2016 *RSC Adv*.***6***, 74903-74912.
[24] TsaiT-Y, HsuC-C, Chao W-K, HuangS-H, ChanC, WuT-C, WangP-H, 2015 *JCCS*,**62**, 6, 562-568.
[25] Mi H-Y, JingX, TurngL-S, 2015 *J. Cell. Plast.*,**51**, n2, 165-196.
[26] Langmuir, I, Langmuir Isotherm, 1916 *JACS*, **38**, 2221–2295.